

AperTO - Archivio Istituzionale Open Access dell'Università di Torino

Photochemical and antioxidant properties of gamma-oryzanol in beta-cyclodextrin-based nanosponges

This is the author's manuscript

Original Citation:

Availability:

This version is available <http://hdl.handle.net/2318/8542> since 2016-08-05T12:25:12Z

Published version:

DOI:10.1007/s10847-012-0147-3

Terms of use:

Open Access

Anyone can freely access the full text of works made available as "Open Access". Works made available under a Creative Commons license can be used according to the terms and conditions of said license. Use of all other works requires consent of the right holder (author or publisher) if not exempted from copyright protection by the applicable law.

(Article begins on next page)



UNIVERSITÀ DEGLI STUDI DI TORINO

This is an author version of the contribution published on:

*Questa è la versione dell'autore dell'opera:
[Journal of Inclusion Phenomena and Macrocyclic Chemistry,
75 (1-2), 2013, 69-76, DOI: 10.1007/s10847-012-0147-3]*

The definitive version is available at:

*La versione definitiva è disponibile alla URL:
[<http://link.springer.com/article/10.1007%2Fs10847-012-0147-3>]*

PHOTOCHEMICAL AND ANTIOXIDANT PROPERTIES OF GAMMA-ORYZANOL IN BETA-CYCLODEXTRIN-BASED NANOSPONGES

S. Sapino¹, M.E. Carlotti¹, R. Cavalli¹, E. Ugazio¹, G. Berlier², L. Gastaldi¹, S. Morel³

¹*Dipartimento di Scienza e Tecnologia del Farmaco, Università degli Studi di Torino, via P. Giuria 9, Torino, 10125, Italy*

²*Dipartimento di Chimica I.F.M., Università degli Studi di Torino and NIS, Nanostructured Interfaces and Surfaces Centre of Excellence, via P. Giuria 7, Torino, 10125, Italy*

³*Dipartimento di Scienze Chimiche, Alimentari, Farmaceutiche e Farmacologiche, Università degli Studi del Piemonte Orientale, via Bovio 6, 28100 Novara, Italy*

Abstract

Gamma-oryzanol (GO), a mixture of ferulic acid esters, has recently attracted a great interest as natural antioxidant extracted from rice-bran oil, usually employed to stabilize food and pharmaceutical raw materials, moreover as sunscreen in cosmetic formulations.

Its usefulness, however, is limited by its fast degradation. A recently proposed approach to increase the stability and effectiveness of antioxidants is based on the inclusion in supramolecular structures (nanoparticles, cyclodextrins, liposomes, etc.). In this work we studied the inclusion of GO in β -cyclodextrin-based nanosponges which in the last few years have been chosen for their ability to encapsulate a great variety of substances to decrease their side-effects and to protect them from degradation. The inclusion complex was prepared in 1:1 w/w ratio and characterized by DSC, XRPD and membrane diffusion runs. The photodegradation of GO upon either UVA or UVB irradiation was found to be slowed down by inclusion in nanosponges. The antioxidant effectiveness of the inclusion complex was also assessed and *in vitro* experiments on porcine ear skin revealed a certain accumulation of GO also when entrapped in the host structure.

Keywords: gamma-oryzanol, nanosponges, photostability, antioxidant effectiveness, skin accumulation

Corresponding author: M.E. Carlotti

Email: eugenia.carlotti@unito.it

Tel: +39(0)116707668

Fax: +39(0)116707687

Introduction

Lipid peroxidation is an oxidative process that occurs by a free radical chain reaction mechanism. It can change the organoleptic and technological properties of oils and fats reducing their self-life. Antioxidants can terminate these chain reactions by removing free radicals, thus they are widely used in foods, pharmaceuticals and cosmetics mostly to inhibit the oxidative degradation of lipid raw materials [1-3]. Moreover, antioxidants have been intensively studied in pharmacology to treat many chronic diseases (atherosclerosis, diabetes, cancer, etc.) [4, 5] and to protect skin against the destructive action of free radicals, produced by UV light and environmental pollutants [6]. Traditionally, synthetic phenolic compounds, such as butylated hydroxytoluene (BHT) and butylated hydroxyanisole (BHA) are widely used as antioxidants in fat-containing formulations, however their harmless is at present a controversial point [7, 8]. Gamma-oryzanol (GO) is a natural antioxidant extracted from rice-bran oil; it contains a mixture of at least ten phytosteryl ferulates among which cycloartenyl ferulate, 24-methylene cycloartanyl ferulate and campesteryl ferulate [9]. It has been reported to possess a wide spectrum of biological activities, in particular it exhibits radical scavenging properties [10], indeed it is used in the treatment of hyperlipoproteinaemias [11] and also in cosmetic formulations as sunscreen [12]. On account of its short term safety, GO has been proposed as a natural antioxidant to improve the stability of foods [3, 13, 14] and vegetable oils of pharmaceutical and cosmetic interest [10]. Unfortunately, it has been reported to be characterized by degradation over time [15]. Particularly, the kinetics of degradation of GO in stripped rice bran oil were investigated under heating at 132, 160, 192 and 222 °C for 480, 140, 60 and 50 hours, respectively. Losses of the overall GO and its components could be expressed by the first-order kinetic model. The rate constant of thermal degradation increased with increasing heating temperatures and the temperature dependence of the obtained rate constants was found to obey the Arrhenius equation.

Recently, increasing attention has been given to solid lipid nanoparticles (SLN) [16] able to protect both lipophilic and hydrophilic drugs against chemical degradation [17]. In literature [18] a study of the incorporation of GO into glycerol behenate (Compritol 888 ATO) SLNs reports that increasing lipid phase concentration resulted in increased consistency and particle diameter of SLNs. Unfortunately, rheological measurement revealed the increase in storage modulus and critical stress during storage at all the studied temperatures 4, 25 and 40 °C. An increase in crystallinity, determined by differential scanning calorimetry, was also found during storage at all temperatures, confirming the instability of SLNs. In the last few years it was reported that, reacting cyclodextrin with suitable cross-linking agent, a nanoporous material was obtained, named nanosponge, which shows interesting performances [19]. It is characterized by the capacity to encapsulate a great variety of substances that can be transported through aqueous media or, from the opposite perspective, removed from contaminated water. The main two characteristics of the nanosponges are the microscopic

and spherical shape of their particles and the polarity of the mesh, that can be tuned through the degree of crosslinking, type of crosslinker and reaction conditions. These characteristics enable the inclusion of several substances, that can be either strongly retained or released in a controlled way. Moreover nanosponges can also decrease side-effects and protect the guest molecule from degradation. GO being a mixture of ferulic acid esters can undergo photolysis [20], accordingly the main objective of this paper was to study the photodegradation of this molecule under UVA and UVB irradiation. Secondly, we examined the possible protective effect on its degradation of the cyclodextrin-based nanosponges where it could be incorporated. The inclusion complex was principally investigated by DSC, XRPD analysis and membrane diffusion. The antiradical and anti-lipoperoxidative activities of GO were also examined to evaluate whether the inclusion in nanosponges could interfere with its antioxidant efficacy. Finally, a study of *in vitro* uptake in ear porcine skin was carried out by comparing free GO with the complex.

Experimental

Materials

Ethanol, methanol, acetonitrile, dichloromethane, 1-butanol and acetic acid were from Carlo Erba (Rodano, Italy) while 1-decanol, 1-dodecanol, sodium azide, sodium dodecyl sulphate (SDS) and phosphoric acid from Fluka (Milan, Italy). GO was obtained from Tsuno Rice Fine Chemicals Co. (Wakayama, Japan) while linoleic acid, 2,2-diphenyl-1-picrylhydrazyl radical (DPPH[•]) and sodium chloride were from Sigma-Aldrich (Milan, Italy). 2-thiobarbituric acid (TBA) and 1,1,3,3-tetraethoxypropane was purchased from Merck (Darmstadt, Germany) while glycerin, hydroxy ethyl cellulose (HEC), octyl octanoate (Tegosoft[®]EE) and polysorbate 20 (Tween[®]20) from A.C.E.F. (Fiorenzuola d'Arda, Italy). Arachidyl alcohol/behenyl alcohol/arachidyl glucoside (Montanov[®]202) was a kind gift from Seppic (Puteaux LaDefense, France) whereas potassium palmitoyl hydrolyzed wheat protein/glyceryl stearate/cetearyl alcohol (Phytocream[®]2000) was supplied by Sinerga (Pero, Italy). β -cyclodextrin (β -CD) based nanosponges (NS) were synthesized in the laboratory of Macromolecular Chemistry according to the procedure reported elsewhere [19]. Briefly, anhydrous β -CD was put to react in melted diphenylcarbonate at 90 °C for 5 h. Once the reaction was complete, the solid was ground in a mortar and Soxhlet-extracted with ethanol to remove unreacted diphenylcarbonate and the phenol produced.

Methods

Analysis of GO

Concentration of GO was determined either by UV spectrophotometry or by HPLC. For UV spectrophotometry, a

standard calibration curve was constructed from the absorbances at 325 nm obtained from GO standard solutions (0.01-0.05 mM) in ethanol ($\epsilon = 35393 \text{ M}^{-1}$). The HPLC system (Shimadzu, Tokyo, Japan) consisted of a LC-6A pump unit control, a SPD-2A UV-Vis detector, a C-R3A chromatopac integrator and a RP-C18 column (Waters, 150×4.6 mm; 5 μm). The mobile phase was a mixture of methanol/acetonitrile/dichloromethane/acetic acid (50/44/3/3 v/v) and its flow rate was kept at 0.8 mL/min. The elution profile was monitored at 325 nm and the retention time of GO was about 15 min. The amount of GO in the sample was quantified, based on the standard curve generated by calculating HPLC peak area of pure GO. Each quantified datum was averaged from triplicate analysis.

Preparation of GO-loaded nanosponges

GO was dispersed in aqueous suspension of NS in a ratio 1:1 by weight and 1.0 mL of ethanol was added to facilitate the dispersion. After 24 h of stirring in the dark the resulting suspension was placed under N_2 flow for 30 min to eliminate ethanol and then freeze-dried to obtain GO-loaded nanosponges (GO/NS). To determinate entrapped drug, weighed amounts of loaded nanosponges were dispersed in ethanol, centrifuged and analyzed by HPLC. For DSC analysis, GO/NS complexes at 1:2 and 1:4 w/w ratio were also prepared following the same procedure above described.

Preparation of GO/NS physical mixtures

Binary physical mixtures of NS with GO were prepared by mixing appropriate amounts of solid components (1:1 weight ratio) in a glass mortar.

Differential scanning calorimetry (DSC)

The measurements were performed by means of a Perkin Elmer DSC/7 differential scanning calorimeter (Perkin Elmer, Waltham, MA, USA). The instrument was calibrated with indium for melting point and heat of fusion. A heating rate of 10 $^{\circ}\text{C}/\text{min}$ was employed in the 100–300 $^{\circ}\text{C}$ temperature range. Standard aluminum sample pans (Perkin-Elmer) were used; an empty pan was used as reference standard. GO and GO/NS complexes at 1:1, 1:2 and 1:4 w/w ratio were analyzed in triplicate under nitrogen purge in the appropriate weight (3-5 mg) such to have the same amount of GO in all of them.

X-ray powder diffraction (XRPD)

Powder XRD patterns were obtained in the range of 1.8-60.0 $^{\circ}$ 2 θ by using a Philips PW1830 (PANalytical, Almelo, Netherlands) X-ray powder diffractometer (Bragg-Brentano geometry) using Ni filtered $\text{CoK}\alpha$ ($\lambda = 1.789 \text{ \AA}$) source at

40 kV and 20 mA in step mode, with a step size of $0.02^\circ 2\theta$ and step time of 6 s/step, with slits of 1° , 1° , and 0.2 mm for scattering, divergence, and receiving respectively, at room temperature.

Preparation of gel and O/W emulsions

The gel was prepared by simply dispersing a weighted amount of HEC (2.0 g) in 98.0 mL of water previously heated at about 80°C . The resultant dispersion was mechanically stirred by a DLS stirrer (Velp Scientifica, Milan, Italy) until a gel was obtained and room temperature was reached.

The first O/W emulsion (E1) was prepared by dispersing under SL-2 homogenizer (Silverson, Bucks, England) the melted lipid phase (6.0 g of Montanov 202 and 15.0 g of Tegosoft EE) in 79.0 mL of water separately heated at about 75°C . Similarly, the second O/W emulsion (E2) was obtained by adding under homogenizer the melted lipid phase (3.0 g of Phytocream 2000 and 14.0 g of Tegosoft EE) to 78.0 mL of hot water containing 5.0 g of glycerin. Both the emulsions were then mechanically stirred by a DLS stirrer until room temperature was reached. A weighted amount of GO, free or complexed with NS, was then added either in HEC gel or in the emulsions under mechanical stirring to achieve the same GO final concentration (1.0 mM).

In vitro release of GO from nanosponges

The apparatus used for the *in vitro* release consisted of two horizontal glass cells of 23.0 mL, with a diameter of 2.4 cm, separated by a membrane filter type AG W-3400 (Sartorius, Göttingen, Germany) impregnated with 1-decanol/1-dodecanol (50/50 v/v). The donor phase consisted of formulation (E1 O/W emulsion) containing a fixed amount of GO (0.06% w/w, 1.0 mM), free or complexed with NS, while the receiving phase was ethanol. At fixed times of 60 min an aliquot (1.0 mL) of the receiving phase was withdrawn, replaced with an equal volume of fresh medium, suitably diluted and analyzed using the HPLC method described previously. The experiment was carried out in triplicate.

GO antiradical activity

The radical scavenging activity of GO free or complexed with NS was determined by the DPPH \cdot free radical assay. Briefly, DPPH \cdot in its radical form absorbs at 515 nm but upon reduction by an antioxidant its absorption decreases [21]. Equal aliquots (20 μL) of dilutions (within the range 0-250 μL) of GO in ethanol or of GO/NS in water were treated with 3.0 mL of DPPH \cdot -saturated ethanol-water (50/50 v/v) solution. The absorbance of each reaction medium was spectrophotometrically monitored at 515 nm after 10 min of incubation under magnetic stirring to reach the steady-state conditions. The DPPH \cdot concentration (mM) was calculated from the calibration curve determined by linear regression

($R^2 = 0.993$):

$$\text{Absorbance} = 10800 \times [\text{DPPH}^*] - 0.0011$$

The percentage of radical scavenging activity (% RSA) of GO in DPPH* solution was calculated according Jang and Xu [22] using the following equation:

$$\% \text{ RSA} = [(A_0 - A_1) / A_0] \times 100$$

where A_0 was the absorbance of DPPH* at zero time and A_1 after 10 min of incubation for the reaction. Each sample was prepared and analyzed in triplicate and the percentage of radical scavenging activity was plotted against each dilution of GO.

GO photostability studies

Photodegradation runs were carried out by irradiating until 60 min the samples placed at 10 cm distance from a BL TL-K 40W UVA lamp (Philips, Milan, Italy) with $6.0 \times 10^{-4} \text{ W cm}^{-2}$ irradiance. During irradiation the samples were stirred by a RO 5 multiple magnetic stirrer (IKA, Staufen, Germany). At scheduled times, a fixed amount (200 μL) of each sample was withdrawn and properly diluted with ethanol for spectrophotometrical analysis. Each sample was prepared at 1.0 mM GO concentration and analysed in triplicate. The samples subjected to irradiation study were: 1) water/ethanol (20/80 v/v) solution containing GO; 2) Tween 20/water (40/60 v/v) mixture containing GO; 3) HEC gel containing GO; 4) HEC gel containing GO/NS; 5) E1 O/W emulsion containing GO; 6) E1 O/W emulsion containing GO/NS.

GO anti-lipoperoxidative activity

The activity of GO against lipoperoxidation was assessed monitoring the levels of malondialdehyde (MDA) generated from lipophilic substrates (linoleic acid or porcine ear skin) upon UVB irradiation by G40T10E lamp (Sankyo Denki, Kanagawa, Japan) with $2.4 \times 10^{-4} \text{ W cm}^{-2}$ irradiance. Since MDA with TBA produces a pink adduct (TBA-MDA-TBA) which absorbs at 535 nm, it can be spectrophotometrically detected according to the method described by Bay et al. [23] with the following modifications. The sample (0.2 mL) was introduced in a glass tube closed with a screw cap and 0.1 mL of water, 0.2 mL of SDS (8.1% w/w), 1.5 mL of phosphoric acid (1.0% w/w) and 1.0 mL of TBA (0.6% w/w) were added. The reaction mixture was heated for 45 min in water bath at 100 °C, then cooled in ice bath and finally 4.0 mL of 1-butanol were added to extract the TBA-MDA-TBA adduct. After centrifugation the absorbance was measured at 535 nm. The final concentration of MDA derived from the reaction was expressed as nmoles of MDA per mg of lipid substrate. A solution of 1,1,3,3-tetraethoxypropane in 8.1% w/w SDS within the concentration range 9.4-208.0 μM was

employed for the calibration curve of the TBA-MDA-TBA complex ($\epsilon = 7098 \text{ M}^{-1}$). MDA can be obtained by acid hydrolysis from 1,1,3,3-tetraethoxypropane in an equimolecular reaction.

Linoleic acid lipoperoxidation

Two SDS solutions (4.0% v/v) containing the same amount of linoleic acid (1.0% w/w) were obtained by adding GO or GO/NS (GO 1.0 mM), respectively. A linoleic acid micellar solution without GO was also prepared as reference. An aliquot (10.0 mL) of each system was transferred in a closed pyrex[®] cell and irradiated for 2 h at a distance of 10 cm from the UVB lamp. After irradiation the linoleic acid dispersions were centrifuged and 0.2 ml of each supernatant was subjected to TBA assay as above described. The experiment was repeated by suspending 1.0 g of linoleic acid in 10.0 g of E2 O/W emulsion, either in the absence or in the presence of GO 1.0 mM, free or complexed with NS.

Porcine skin lipoperoxidation

Skin slices were isolated by a GA 643 Acculan dermatome (Aesculap, Tuttlingen, Germany) from pig ears freshly obtained from a local slaughterhouse and frozen at $-18 \text{ }^{\circ}\text{C}$ for at least 24 h. Before the experiments the slices were pre-equilibrated in 0.9% w/w saline solution, added with sodium azide to preserve the skin, at $25 \text{ }^{\circ}\text{C}$ for 30 min and further cut up in small pieces that were mixed to overcome a possible variability among different zones of the ear skin. The pieces (total weight 2.3-2.5 g) were randomly allocated in pyrex[®] cells, suspended in 4.0% w/w SDS solution and irradiated (2 h) by UVB lamp either in the absence and in the presence of GO (1.0 mM), free or complexed with NS. After irradiation the skin pieces were dried under vacuum and then incubated for 16 h in 10.0 mL dichloromethane under magnetic stirring to extract MDA. The organic solvent was then evaporated under vacuum by RE-111 Rotavapor (Büchi, Flawil, Switzerland) and the residue was reconstituted with 3.0 mL of 8.1% w/w SDS. An aliquot (0.2 mL) of this dispersion was subjected to the TBA assay by means of the same procedure reported above. The experiment was repeated by suspending the same quantity of skin pieces (total weight 2.3-2.5 g) in 10 g of E2 O/W emulsion either in the absence and in the presence of GO (free or complexed with NS) and then following the same procedure just described.

In vitro GO skin accumulation

Skin slices were isolated by dermatome from pig ears, frozen at $-18 \text{ }^{\circ}\text{C}$ and treated as above reported for skin lipoperoxidation studies. A piece of excised skin slice, previously defrosted and equilibrated in saline solution, was mounted with the *stratum corneum* side facing towards the donor compartment of a Franz diffusion cell. The available

area of the cell was around 1.6 cm^2 . The donor compartment was filled alternatively with: *i*) GO (1.0 mM) in 4.0% w/w SDS solution (pH 5.0); *ii*) GO/NS (GO 1.0 mM) in 4.0% w/w SDS solution (pH 5.0); *iii*) GO (1.0 mM) in E2 O/W emulsion; *iv*) GO/NS (GO 1.0 mM) in E2 O/W emulsion. The receptor compartment was filled with saline solution and magnetically stirred at $37 \text{ }^\circ\text{C}$. The amount of GO retained in the skin was determined at the end of the experiment (24 h) as follows: the application site on the skin was washed with water/ethanol (50/50 v/v) mixture, cut in small pieces by scissor and extracted with 3.0 mL of ethanol. After 2 h of magnetic stirring the resulting suspension was centrifuged and assayed by spectrophotometer. The skin accumulation was expressed as amount of GO on skin diffusion area ($\mu\text{g cm}^{-2}$).

Results and discussion

DSC studies

The interaction between GO and NS was confirmed by DSC analysis. Firstly, the thermogram of nanosponges showed no peak before $320 \text{ }^\circ\text{C}$ (data not shown), meaning that this material has high thermal stability. Moreover, as shown in Fig. 1 the thermogram of pure GO displayed one broadened endothermic peak around $167 \text{ }^\circ\text{C}$. When GO/NS complexes in different ratios were analyzed, a marked reduction in transition enthalpy of GO (11.537 J g^{-1}) was observed even if an endothermic transition was still present in all of them. This indicates that a certain interaction between the two substances occurred. Particularly, from the thermograms it can be observed that GO was loaded in the highest amount in 1:4 w/w GO/NS complex as much as 78.3%, with loadings of 56.4% and 32.2% in 1:2 and 1:1 w/w samples, respectively.

Fig. 1 DSC thermograms of GO and GO/NS complexes in different weight ratios (1:1, 1:2 and 1:4 w/w)

X-ray powder diffraction (XRPD)

The host-guest interaction and structure of the resulting complex was studied by X-ray powder diffraction. In Fig. 2 the XRD pattern of GO/NS is compared to those of NS, GO and of a physical mixture of the two, while the inset reports the magnification of the main peaks of GO, GO/NS complex and of physical mixture (solid, dashed and dotted curves, respectively). These data show that GO preserves its crystalline structure interacting with the nanosponges, which in turn show a weak long range order characterized by some broad reflections (5.1 , 14.0 and $22.1^\circ 2\theta$) [24]. The physical mixture XRD pattern shows the GO peaks superimposed to those related to the poorly crystalline NS. On the contrary, in the GO/NS complex the broad peaks due to the paracrystalline NS [24] are consumed, and those due to the crystalline GO structure are shifted to lower 2θ (see inset). This indicates an interaction between GO and the nanosponges.

Fig. 2 Powder XRD patterns of GO, GO/NS complex, nanosponges and a physical mixture of the two. The inset reports a magnification of the main peaks of GO (solid line), GO/NS (dashed line) and physical mixture (dotted line) arbitrarily normalized and vertically shifted for easier comparison

In vitro release of GO from nanosponges

GO and nanosponges association was also studied by evaluating the diffusion through an artificial lipophilic membrane. The choice of this barrier was justified by the structural characteristic of GO and because it is impermeable to the host molecule. The purpose of the present study was to investigate the effect of nanosponges on the permeability of GO through the membrane to further confirm its interaction with nanosponges. *In vitro* diffusion studies showed that the GO release kinetics, after an initial burst effect (60 min), was of pseudo-zero order ($y = 0.071x + 18.51$; $R^2 = 0.993$). Likewise diffusion of GO/NS followed a pseudo-zero order kinetics and exhibited a high initial release, but in comparison with free GO it was slightly delayed ($y = 0.052x + 16.48$; $R^2 = 0.999$) confirming a certain interaction between the two materials.

Fig. 3 Amounts ($\mu\text{g}/\text{cm}^2$) of GO and GO/NS diffused over time through the lipophilic membrane. Each bar represents the mean \pm SD obtained in three independent experiments (n=3)

GO antiradical activity

The reaction with DPPH[•] is widely used for assessing the ability of polyphenols to transfer labile atoms to radicals, a common mechanism of antioxidant protection [21]. This assay is based on the reduction of DPPH[•] which causes an absorbance decrease at 515 nm after acceptance of an electron or hydrogen radical from an antioxidant compound. Accordingly, in this study the antioxidant activity of GO was evaluated from the remaining DPPH[•] when the kinetics reached the steady-state as a function of the molar concentration of the antioxidant. Fig. 4 illustrates that the scavenging effect (% RSA) of GO increased with increasing GO concentration. The radical scavenging activity of GO/NS complex slightly differed from that of free GO. In fact in the presence of low amounts of GO the % RSA of GO/NS was slightly lower than that of free GO whereas with higher concentration ($> 150 \mu\text{M}$) trend is reversed.

Fig. 4 Radical scavenging activity (% RSA) of GO, free or complexed with NS, towards DPPH[•]. Each bar represents the mean \pm SD obtained in three independent experiments (n=3)

Photodegradation studies

GO absorbs in the UV region displaying a peak around 325 nm whose intensity decreases upon UVA irradiation indicating a photolysis process of this molecule.

In the following irradiation runs the photodegradation kinetics of free GO and GO/NS complex were compared in order to investigate the protective effect of the nanosponges on the photooxidation of the guest molecule. Moreover, the influence of the media (hydroalcoholic solution, micellar solution, gel and O/W emulsion) was examined as our recent results indicated that the photooxidation rates can be influenced by the polarity of the medium [25-26].

The photodegradation kinetics was studied by plotting GO concentration as a function of irradiation time (in minutes). The curves (data non reported) show an exponential asymptotic trend which denotes that in all the media GO degraded upon UVA illumination according a first order kinetic. The slope of the curves was calculated by the logarithmic equation:

$$\ln C_t/C_o = -k \times t$$

where C_o is the initial concentration of organic molecule and C_t represents its residual concentration at time t . The linear dependence of $\ln C_t/C_o$ versus time can be used to obtain the data of rate constant. Using the fittings of pseudo-first order model, the values of k were listed in Table 1. A comparison of the rate constants of photodegradation obtained in different media indicates that GO rate of degradation increases following this sequence: O/W emulsion < Tween 20/water < water/ethanol < HEC gel. This finding confirms our previous data [25-26] according to which environments with low polarity (emulsion or micelles) are able to restrict photooxidation process. On the basis of measured kinetic parameters it can be noted that the photodegradation rate of GO complexed with NS is slower than that of free one, confirming that the complexation phenomenon provides GO with a physical barrier against UV-induced oxidation.

Table 1. Rate constants (k) and correlation coefficients (R^2) of GO (free or complexed with NS) photodegradation in different media under UVA irradiation

	GO		GO/NS	
	$k \times 10^3$ (min ⁻¹)	R^2	$k \times 10^3$ (min ⁻¹)	R^2
Water/ethanol (20/80 v/v)	7.8 ± 0.4	0.995	-	-
Tween 20/water (40/60 v/v)	6.2 ± 0.1	0.819	-	-
HEC gel	11.8 ± 0.5	0.994	3.1 ± 0.1	0.971
O/W emulsion (E1)	5.3 ± 0.3	0.881	0.6 ± 0.1	0.843

GO anti-lipoperoxidative activity

This experiment was designed to assess the preventive effect of GO against the damages of UVB radiation towards lipid substrates, particularly the skin lipids. Because lipoperoxidation is regarded as a marker of oxidative stress, we evaluated this phenomenon by monitoring the formation of MDA from the lipid substrate. The protective effect of GO was tested firstly on a simple lipid substrate, linoleic acid, and then on porcine ear skin, a more complex substrate considered being the closest to human skin [27]. Fig. 5 a, b reports the values of MDA formed from linoleic acid and from ear porcine skin, respectively. It can be observed that the presence of GO was found to inhibit the lipoperoxidation induced by UVB irradiation for both the lipid substrates, both in micellar solution and in E2 O/W emulsion. Besides, it can be noted that GO presents a significant anti-lipoperoxidative activity also when it is complexed with the nanosponges.

Fig. 5 a, b Amounts of MDA derived from lipid substrate (**a.** linoleic acid; **b.** porcine ear skin samples), in SDS solution or in O/W emulsion (E2), after 2 h of UVB irradiation in the absence and in the presence of GO (1.0 mM), free or complexed with NS. Each bar represents the means \pm SD obtained in three independent experiments (n=3)

In vitro GO skin accumulation

As above reported GO can be employed in topical formulations as antioxidant and sunscreen, therefore it can be interesting to investigate its skin permeation. This experiment allowed to determine *in vitro* the amount of GO, free or complexed with NS, which is accumulated in the porcine skin. A negligible percutaneous accumulation within 24 h was observed in all the receiving phase, while the amounts of GO accumulated in the skin 24 h after application are presented in Table 2.

It can be noted that in SDS micellar solution free GO and GO/NS gave skin accumulation of 57.1 and 65.8 $\mu\text{g cm}^{-2}$, respectively, meanwhile for O/W emulsion (E2) lower GO accumulation levels were observed (1.5 $\mu\text{g/cm}^2$ for free GO and 2.3 $\mu\text{g cm}^{-2}$ for GO/NS).

The ability of NS inclusion to increase the skin uptake of the guest, observed in both the media, could be linked to the fact that cyclodextrins, as already reported, can enhance drug permeation mainly by increasing its solubility at the lipophilic surface of the skin [28, 29]. Moreover, Table 2 shows that GO skin uptake levels resulted higher from micellar solution than from O/W emulsion (E2), reasonably because SDS acts as enhancer of permeation.

Table 2. GO accumulation in porcine ear skin, 24 h after application

Sample	Accumulation ($\mu\text{g cm}^{-2}$)
GO in SDS solution	57.1 ± 3.2
GO/NS in SDS solution	65.8 ± 4.1
GO in O/W emulsion (E2)	1.5 ± 0.8
GO/NS in O/W emulsion (E2)	2.3 ± 0.7

Conclusions

In this paper an inclusion complex between GO and cyclodextrin-based nanosponges was investigated. DSC thermograms and powder XRD patterns together with the diffusion studies suggested the formation of the inclusion complex. On the basis of measured kinetic parameters the complexation protects GO from UV photodegradation without significantly limiting its antioxidant properties. Furthermore *in vitro* studies performed on Franz diffusion cells demonstrated that the complexation phenomenon does not inhibit the accumulation of GO in porcine ear skin. In conclusion the formation of NS inclusion complex with GO provides an indication that it may have potential as carrier for topically active substances..

Acknowledgments

Authors want to thank Prof. F. Trotta for his kindness in providing the β -CD based nanosponges.

References

- [1] Lupo, M.P.: Antioxidants and vitamins in cosmetics. *Clin. Dermatol.* 19, 467-473 (2001)
- [2] German, J.B.: Food processing and lipid oxidation. *Adv. Exp. Med. Biol.* 459, 23-50 (1999)
- [3] Nanua, J.N., Mc Gregor, J.U., Godber, J.S.: Influences of high oryzanol rice bran oil on the oxidative stability of whole milk powder. *J. Dairy Sci.* 83, 2426-2431 (2000)
- [4] Willcox, J.K., Ash, S.L., Catignani, G.L.: Antioxidants and prevention of chronic disease. *Crit. Rev. Food Sci. Nutr.* 44, 275-295 (2004)
- [5] Ito, N., Hirose, M., Fukushima, S., Tsuda, H., Shirai, T., Tatematsu, M.: Studies on antioxidants: their carcinogenic and modifying effects on chemical carcinogenesis. *Food Chem. Toxicol.* 24, 1071-1082 (1986)
- [6] Burke, K.E.: Photodamage of the skin: protection and reversal with topical antioxidants. *J. Cosm. Dermatol.* 3, 149-155 (2004)

- [7] Whysner, J., Wang, C.X., Zang, E., Iatropoulos, M.J., Williams, G.M.: Dose response of promotion by butylated hydroxyanisole in chemically initiated tumors in the rat forestomach. *Food Chem. Toxicol.* 32, 215-222 (1994)
- [8] Williams, G.M., Iatropoulos, M.J., Whysner, J.: Safety assessment of butylated hydroxyanisole and butylated hydroxytoluene as antioxidant food additives. *Food Chem. Toxicol.* 37, 1027-1038 (1999)
- [9] Xu, Z., Godber, J.S.: Purification and identification of components of γ -oryzanol in rice bran oil. *J. Agric. Food Chem.* 47, 2724-2728 (1999)
- [10] Juliano, C., Cossu, M., Alamanni, M., Piu, L.: Antioxidant activity of gamma-oryzanol: mechanism of action and its effect on oxidative stability of pharmaceutical oils. *Int. J. Pharm.* 299, 146-154 (2005)
- [11] Cicero, A.F., Gaddi, A.: Rice bran oil and gamma-oryzanol in the treatment of hyperlipoproteinaemias and other conditions. *Phytother. Res.* 15, 277-89 (2001)
- [12] Coppini, D., Paganizzi, P., Santi, P., Ghirardini, A.: Capacità protettiva nei confronti delle radiazioni solari di derivati di origine vegetale. *Cosmetic News* 136, 15-20 (2001)
- [13] Chotimarkou, C., Nemjakul, S., Silalai, N.: Antioxidative effects of rice bran extracts on refined tuna oil during storage. *Food Res. Intern.* 41, 616-622 (2008)
- [14] Renuka Devi, R., Jayalekshmy, A., Arumughan, C.: Antioxidant efficacy of phytochemical extracts from defatted rice bran in bulk oil system. *Food Chem.* 104, 658-664 (2007)
- [15] Khuwijtjaru, P., Yuenyong, T., Pongsawatmanit, R., Adachi, S.: Degradation kinetics of gamma-oryzanol in antioxidant-stripped rice bran oil during thermal oxidation. *J. Oleo Sci.* 58, 491-497 (2009)
- [16] Müller, R.H., Mäder, K., Gohla, S.: Solid lipid nanoparticles (SLN) for controlled drug delivery-a review of the state of the art. *Eur. J. Pharm. Biopharm.* 50, 161-177 (2000)
- [17] Wissing, S.A., Müller, R.H.: Solid lipid nanoparticles as carrier for sunscreen: in vitro release and in vivo skin penetration. *J. Control. Release* 81, 225-233 (2002)
- [18] Seetapan, N., Bejrappa, P., Srinuanchai, W., Ruktanonchai, U.R.: Rheological and morphological characterizations on physical stability of gamma-oryzanol-loaded solid lipid nanoparticles (SLNs). *Micron* 41, 51-58 (2010)
- [19] Cavalli, R., Trotta, F., Tumiatti, W.: Cyclodextrins-based nanosponges for drug delivery. *J. Incl. Phenom. Macrocycl. Chem.* 56, 209-213 (2006)
- [20] Carlotti, M.E., Sapino, S., Ugazio, E., Peira, E., Vione, D., Minero, C.: Photostability of ferulic acid and its antioxidant activity against linoleic acid peroxidation. *J. Disp. Sci. Technol.* 29, 629-640 (2008)
- [21] Brand-Williams, W., Cuvelier, M.E., Berset, C.: Use of a free radical method to evaluate antioxidant activity. *Food Sci. Tech.* 28, 25-30 (1995)

- [22] Jang S., Xu Z.: Lipophilic and hydrophilic antioxidants and their antioxidant activities in purple rice bran. *J. Agric. Food Chem.* 57, 858-862 (2009)
- [23] Bay, B.-H., Lee, Y.-K., Tan, B.K.-H., Ling, E.-A.: Lipid peroxidative stress and antioxidative enzymes in brains of milk-supplemented rats. *Neurosci. Lett.* 277, 127-133 (1999)
- [24] Swaminathan, S., Pastero, L., Serpe, L., Trotta, F., Vavia, P., Aquilano, D. Trotta, M., Zara, G.P., Cavalli, R.: Cyclodextrin-based nanosponges encapsulating camptothecin: physicochemical characterization, stability and cytotoxicity. *Eur. J. Pharm. Biopharm.* 74, 193-201 (2010)
- [25] Carlotti, M.E., Sapino, S., Vione, D., Pelizzetti, E., Trotta, M.: Photostability of Trolox in water/ethanol, water and Oramix CG110, in the absence and in the presence of TiO₂. *J. Disp. Sci. Technol.* 25, 193-207 (2004)
- [26] Carlotti, M.E., Sapino, S., Vione, D., Minero, C., Peira, E., Trotta, M.: Study on the photodegradation of salicylic acid in different vehicles in the absence and in the presence of TiO₂. *J. Disp. Sci. Technol.* 28, 805-818 (2007)
- [27] Jacobi, U., Kaiser, M., Toll, R., Mangelosdorf, S., Audring, H., Otberg, N., Sterry, W., Lademann, J.: Porcine ear skin: an in vitro model for human skin. *Skin Res. Technol.* 13, 19-24 (2007)
- [28] Sapino, S., Carlotti, M.E., Caron, G., Ugazio, E., Cavalli, R.: *In silico* design, photostability and biological properties of the complex resveratrol/hydroxypropyl- β -cyclodextrin. *J. Incl. Phenom. Macrocycl. Chem.* 63, 171-180 (2009)
- [29] Godwin, D.A., Wiley, C.J., Felton, L.A.: Using cyclodextrin complexation to enhance secondary photoprotection of topically applied ibuprofen. *Eur. J. Pharma. Bipharma.* 62, 85-93 (2006)

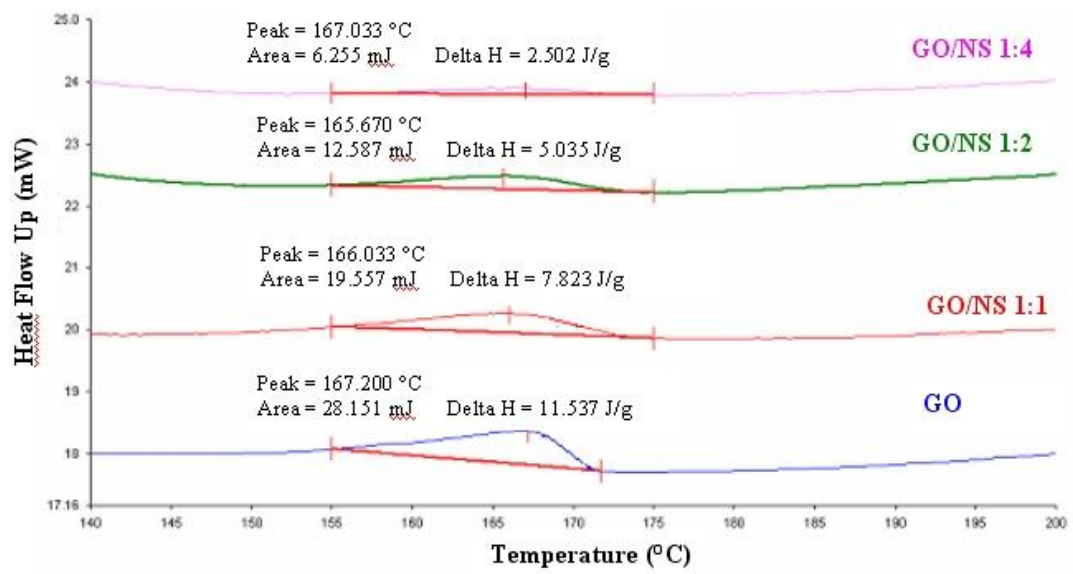


Fig. 1

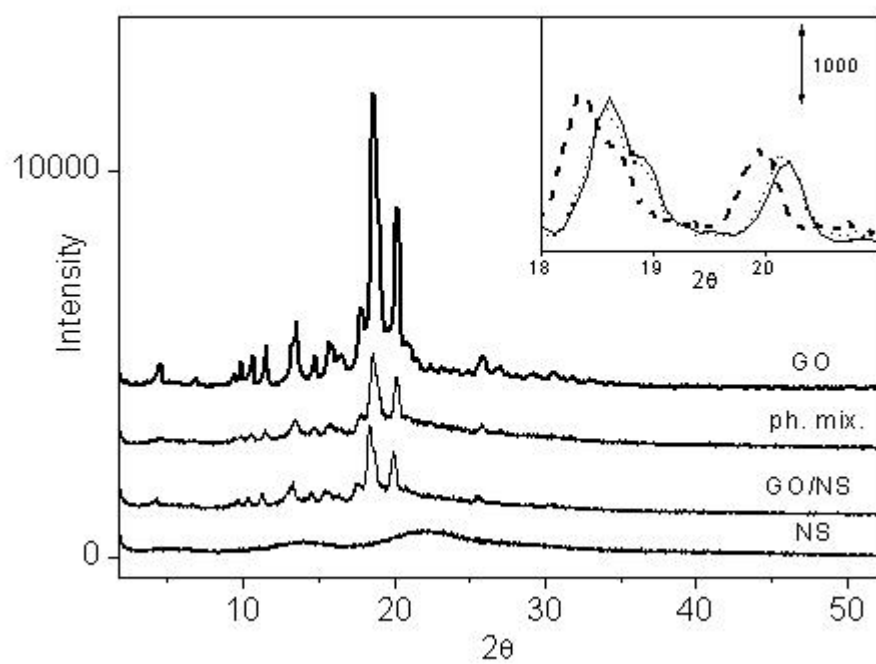


Fig. 2

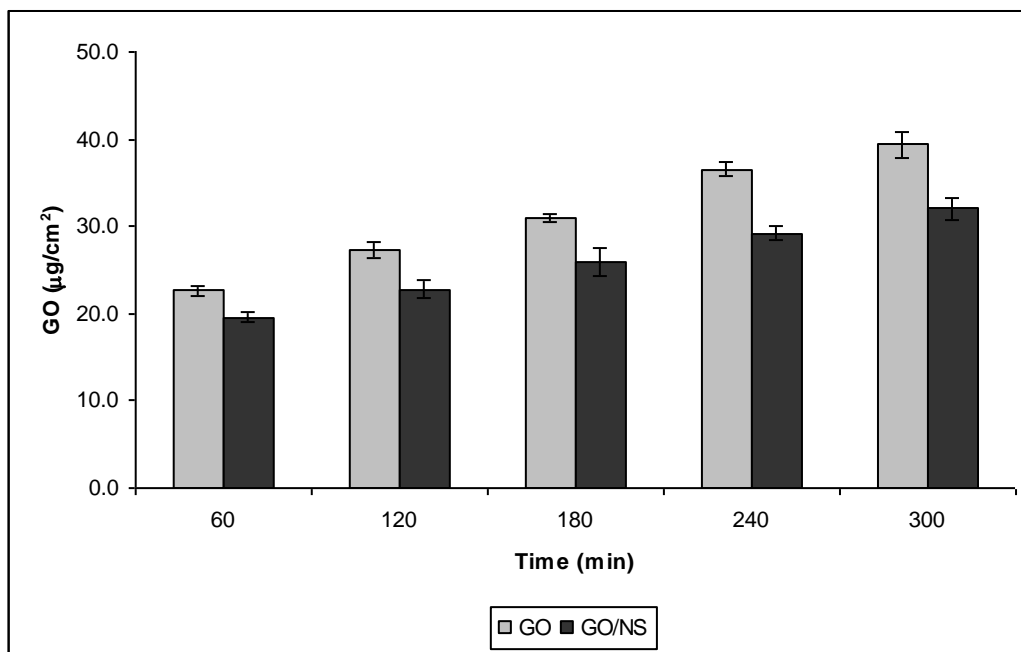


Fig. 3

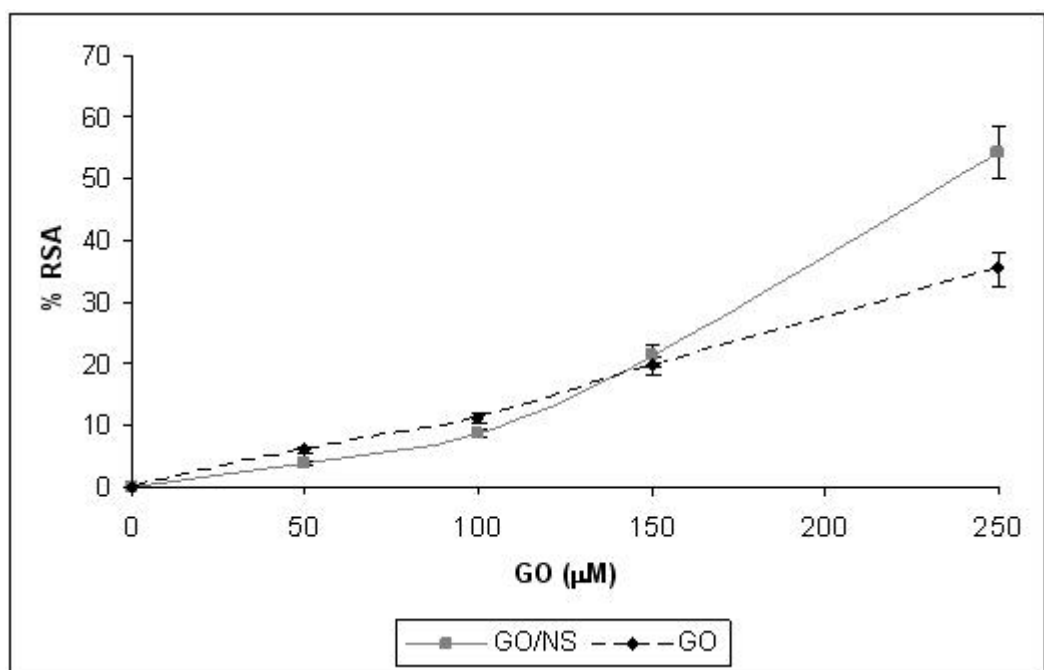
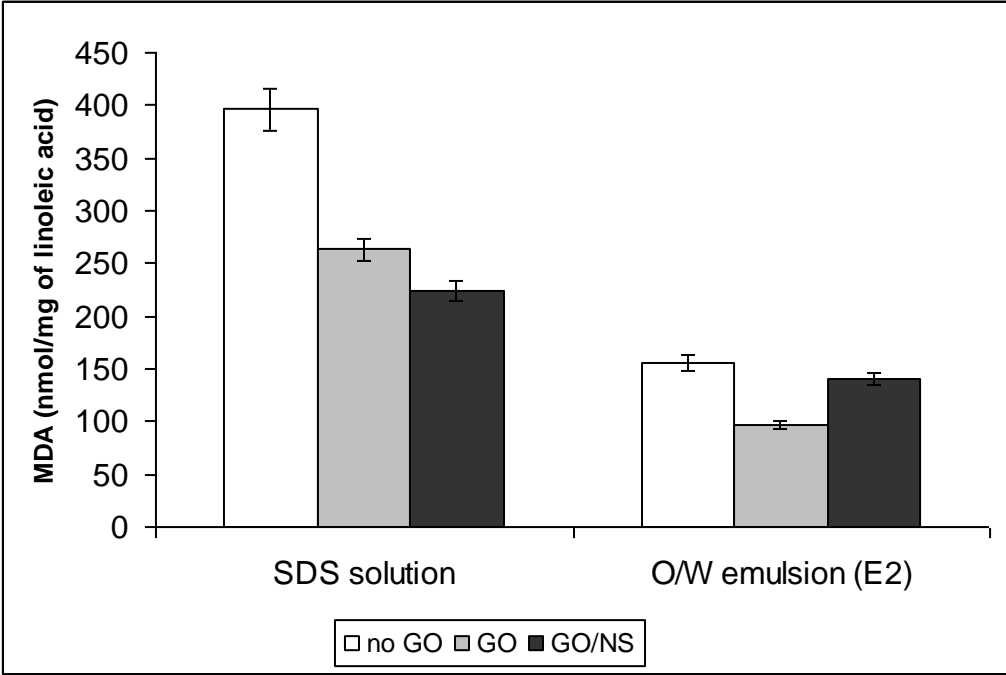
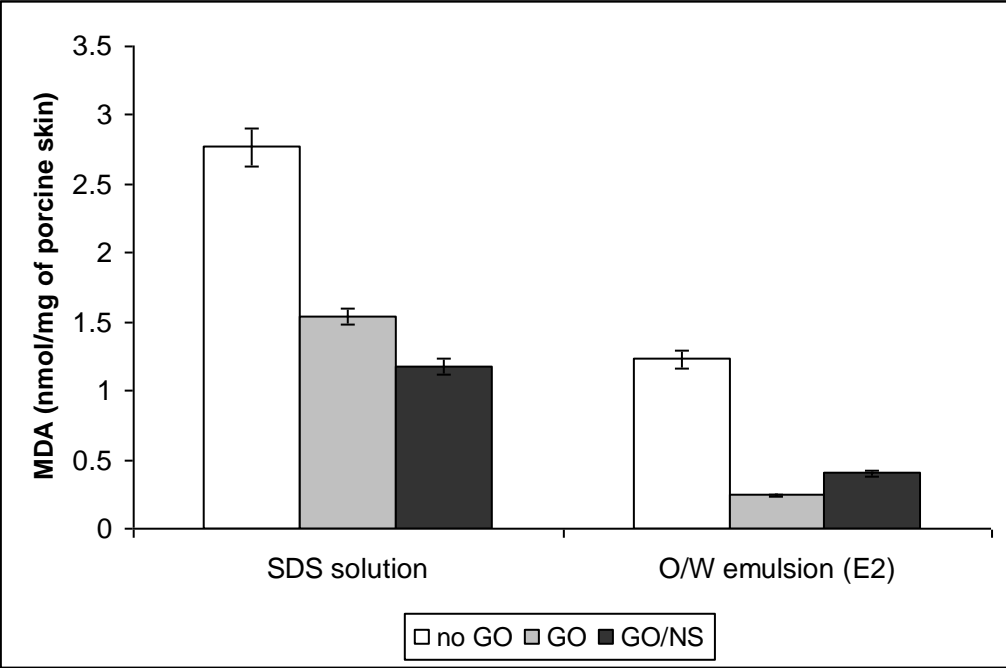


Fig. 4



a



b

Fig. 5